Available online at www.sciencedirect.com
ScienceDirect
Journal of Power Sources 164 (2007) 365–371
JOURNAL OF POWER SOURCES
www.elsevier.com/locate/jpowsour

Diffusion-limited model for a lithium/air battery with an organic electrolyte

S.S. Sandhu [a,*], J.P. Fellner [b], G.W. Brutchen [a]

[a] *Department of Chemical and Materials Engineering, University of Dayton, 300 College Park, Dayton, OH 45469-0246, United States*
[b] *Air Force Research Laboratory, Propulsion Directorate, Plans and Analysis Branch, 1950 Fifth Street, Wright-Patterson AFB, OH 45433-7251, United States*

Received 18 August 2006; received in revised form 30 August 2006; accepted 16 September 2006
Available online 15 November 2006

Abstract

A diffusion-limited transient mathematical model for a lithium/air cell, with the air cathode pores flooded with an organic electrolyte, has been developed. During cell discharge, the cathode pore radius profile is reflective of the distribution of the lithium peroxide product in the cathode. The cathode pore radius profile has been predicted as a function of time, current density, oxygen gas pressure, and cathode thickness for an assumed initial porosity and average cathode pore size. Transient concentration profiles of the dissolved oxygen in the electrolyte were also determined. Capacities of the lithium/air cell were predicted and compared favorably with literature experimental results.

Keywords: Lithium/air cell; Transient model; Organic electrolyte; Diffusion-limited

1. Background

Metal/air batteries are unique in that the air cathode active material, oxygen, is not stored internal to the cell/battery system. Oxygen is provided by access of air to the porous carbon cathode electrode for the half-cell oxygen reduction process. Table 1 shows the characteristics of some metal/oxygen battery couples as given by Abraham and Jiang [1].

From Table 1 it is obvious that the lithium/oxygen battery has the highest theoretical specific energy. However, as the battery discharge process progresses, the metal/air batteries get heavier with time, thus the true theoretical specific energy for this type of battery for the entire discharge period is the average of the values of the "excluding O_2" and that of "including O_2". For lithium/oxygen, this average theoretical energy density is 8170 Wh kg^{-1}. This value is higher than the heat of combustion lower heating value (LHV) energy density of 5524 Wh kg^{-1} for methanol/air, but, less than the LHV energy density of 11,860 Wh kg^{-1} for gasoline/air [2]. Thus, with metal/air batteries typically achieving 33% of their theoretical specific energy values or higher, this type of battery has the potential to be the lightest power source for powering portable electronic equipment, unmanned aerial vehicles, camping equipment, or any equipment where air is present [3].

The lithium/oxygen organic electrolyte battery differs from the aqueous metal/air batteries in that the oxygen reduction product is insoluble in the organic polymer electrolytes [1,4,5]. Work performed using a rechargeable lithium/oxygen battery, using a lithium ion conducting organic polymer electrolyte, led to the conclusion that the primary cell reaction is given by the following equation [1]:

$$2Li_{(s)} + O_{2(g)} \rightleftharpoons Li_2O_{2(s)} \quad (1)$$

From the oxygen consumption measurements and experimental data analysis [4], the reaction given by Eq. (2) was found to also occur during the lithium/air cell discharge for certain organic electrolytes and at higher discharge rates

$$2Li_{(s)} + \tfrac{1}{2}O_{2(g)} \rightleftharpoons Li_2O_{(s)} \quad (2)$$

Read et al. [4,5] have shown that for a given flooded-electrolyte design, the organic electrolyte formulation and the oxygen concentration have the largest effects on the battery discharge capacity and rate capability. It was concluded that the cells

* Corresponding author. Tel.: +1 937 229 2648.
E-mail address: Sarwan.Sandhu@notes.udayton.edu (S.S. Sandhu).

0378-7753/$ – see front matter © 2006 Elsevier B.V. All rights reserved.
doi:10.1016/j.jpowsour.2006.09.099

Table 1
Characteristics of some metal/oxygen battery couples

Metal/O_2 couple	Ideal cell reaction[a]	Calculated open-circuit voltage at 25 °C (V)	Theoretical specific energy[b] (Wh kg^{-1})	
			Including O_2	Excluding O_2
Li/O_2	$4Li + O_2 \rightleftharpoons 2Li_2O$	2.91	5200	11,140
Al/O_2	$4Al + 3O_2 \rightleftharpoons 2Al_2O_3$	2.73	4300	8,130
Ca/O_2	$2Ca + O_2 \rightleftharpoons 2CaO$	3.12	2990	4,180
Zn/O_2	$2Zn + O_2 \rightleftharpoons 2ZnO$	1.65	1090	1,350

[a] The reduction of O_2 to O^{2-} usually occurs only in the presence of a catalyst; often the product is the peroxide, O_2^{2-}.
[b] Includes only the active materials. Since O_2 does not have to be carried in the battery, values are given for the cases of including and excluding O_2. The battery weight will increase once the discharge begins.

were limited by oxygen diffusion and that dissolved oxygen diffusivity and concentration are of critical importance for the performance of a lithium/air or oxygen flooded-electrolyte cell. Oxygen concentration in an organic electrolyte is dependent on the electrolyte formulation and gaseous oxygen partial pressure. Ways to enhance the dissolved oxygen diffusivity and concentration in the organic electrolyte were by the use of different electrolyte formulations and by the increase of the gaseous oxygen partial pressure.

Metal catalysts in the carbon/air cathodes were employed [3] to enhance the practical energy density of the lithium/air battery. The catalysts investigated were: manganese (Mn), cobalt (Co), ruthenium (Ru), platinum (Pt), silver (Ag), and a mixture of Co and Mn. The Mn catalyzed carbon cathodes showed the best performance followed by the Co catalyzed carbon cathodes. The specific discharge capacity of the Mn catalyzed carbon cathodes was determined to be 3137 mAh g^{-1} of carbon at a discharge rate of 0.1 mA/cm^2_{geom} at a cut-off voltage of 1.5 V, whereas the Co catalyzed carbon cathode capacity was 2414 mAh g^{-1} of carbon.

Using in situ mass spectrometry [6], it has been shown that the electrochemical reaction given by Eq. (1) in a nonaqueous electrolyte, such as 1 M $LiPF_6$ in propylene carbonate (PC), is reversible and charge/discharge cycling can be carried out. The fundamental and practical issues are: the role of electrochemical manganese dioxide and other transition metal compounds in promoting the cathode electrode reaction, optimization of electrode porosity, structure, and composition of the cathode electrode. Prevention of water or carbon dioxide from entering the cell, when operated in air, is also a very important issue.

A preliminary analysis of the lithium/air battery system was performed [7]. In this analysis, the reversible, individual electrode and overall cell reaction voltages for the formation of only $Li_2O_{2(s)}$ and both $Li_2O_{(s)}$ and $Li_2O_{2(s)}$ as the solid discharge product species in the air cathode reaction layer, amounts of the chemical species $Li_2O_{2(s)}$, $Li_2O_{(s)}$, and $Li_{(s)}$ as a function of cell discharge time, and the theoretical discharge capacity and thermal efficiency of the cell were determined. The total composite cathode volume for a desired maximum cell discharge, pore volume, and volumes of the carbon and lithium peroxide materials were computed using developed analytical expressions. A mathematical expression, based on the first law of thermodynamics, to compute heat exchange between the lithium cell or battery and its surroundings was also developed.

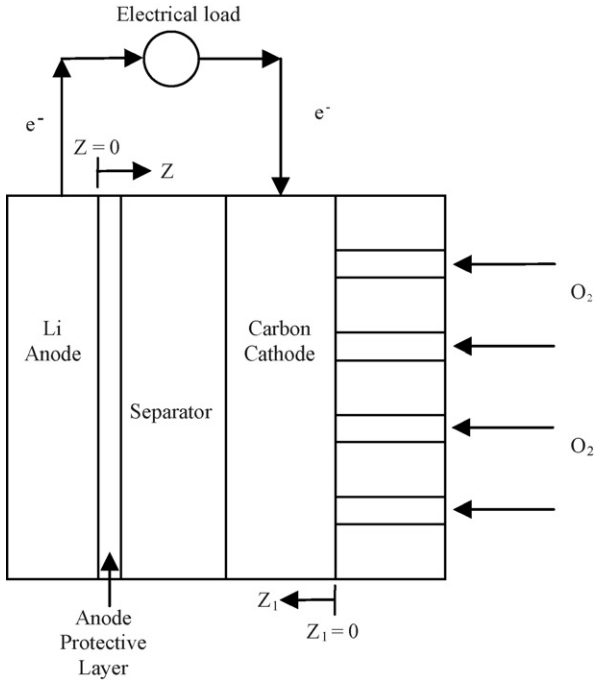

Fig. 1. Simple sketch of lithium/air system.

The formulation presented in this paper is for a lithium/air cell, consisting of a thin lithium sheet anode, lithium phosphorous oxynitride (LiPON) or glass anode protective layer, and a porous carbon oxygen/air cathode; see Fig. 1. The porous carbon cathode is assumed to be made of carbon black, catalyzed by a metal such as manganese, polytetrafluoroethylene (PTFE) as the binder, and the pores are flooded with a lithium based electrolyte, for example, 1 M $LiPF_6$ in PC/1,2-dimethoxyethane (DME) in a mass ratio of 1:1 (1:1).

2. Mathematical formulation

Dependence of the lithium/air system performance on oxygen solubility, concentration, and its transport in organic electrolytes was experimentally shown [4,5]. A diffusion-limited model for oxygen transport and its conversion in the porous cathode reaction layer is presented below.

Due to the low current densities, voltage losses associated with current collection, the lithium anode half-cell reaction, and lithium ion transport in the electrolyte are assumed to be

minimal. The flooded-electrolyte cell is assumed to be diffusion-limited with respect to dissolved oxygen. The porous carbon cathode is assumed to be catalyzed by a catalytic agent, for example, manganese (Mn). Pores in the carbon reaction layer are assumed to be full of the liquid phase electrolyte such as 1 M solution of $LiPF_6$ in an organic solvent mixture, e.g., PC/DME (1:1). The electrolyte has an initial concentration of dissolved oxygen. This initial oxygen concentration may be equal to zero (i.e. no oxygen present in the electrolyte) or equal to the solubility limit (i.e. saturated concentration of oxygen at the prevailing temperature and pressure conditions). Furthermore, the condition of isothermality is assumed to prevail. During the cell discharge, oxygen diffuses through the liquid phase electrolyte in pores from the pure oxygen or air side of the cathode towards its side in contact with the lithium anode protective layer, for example, the LiPON or glass layer; assuming that the thickness of electrolyte separator layer between the protected anode and cathode is negligibly small. Oxygen is consumed by its reaction with the lithium ions in the presence of electrons at the active sites located at the carbon–electrolyte interface. It is assumed that the lithium ion concentration in the electrolyte solution is sufficiently high so that the electrochemical oxygen reduction can be safely assumed to be pseudo first-order with respect to the dissolved oxygen concentration. The developed oxygen continuity equation, describing oxygen transport and its reduction in the porous carbon cathode, is given below

$$\frac{\partial}{\partial t}(\varepsilon c_{\mathrm{A}}) = \frac{\partial}{\partial z_1}\left(\frac{D_{\mathrm{A}}\varepsilon}{\tau}\frac{\partial c_{\mathrm{A}}}{\partial z_1}\right) - R_{\mathrm{A}} \tag{3}$$

where ε is the electrolyte filled pore volume fraction in the cathode reaction layer, $c_{\mathrm{A}} = c_{\mathrm{O_2}}$ is the oxygen molar concentration in the liquid phase electrolyte, τ is the cathode pore tortuosity factor, and D_{A} is the oxygen mass diffusivity in the liquid phase electrolyte. The oxygen conversion rate, R_{A}, at the active sites located at the pores surfaces per unit cathode volume is given by

$$R_{\mathrm{A}} = \left(\frac{2\varepsilon}{\bar{r}_{\mathrm{p}}}\right) k_{\mathrm{s}} c_{\mathrm{A}} = 2k_{\mathrm{s}}\left(\frac{\varepsilon}{\bar{r}_{\mathrm{p}}} c_{\mathrm{A}}\right) \tag{4}$$

where k_{s} is the overall electrochemical oxygen reduction rate coefficient at a given cell operational temperature, and $\bar{r}_{\mathrm{p}}$ is the mean pore radius of pores filled with the electrolyte solution. In the derivation of Eq. (3), it has been assumed that $\partial c_{\mathrm{A}}/\partial r \cong 0$ (i.e. pores are sufficiently narrow), and $\partial c_{\mathrm{A}}/\partial\theta = 0$ (symmetry with respect to the angular coordinate θ around the axis of a pore). Note that here

$$k_{\mathrm{s}} = k_{\mathrm{s,e}} \exp\left(\frac{|\eta^{\mathrm{c}}|\alpha^{\mathrm{c}} F}{RT}\right) = \left[k_{\mathrm{s,e,0}} \exp\left(\frac{-E_{\circ}}{RT}\right)\right] \exp\left(\frac{|\eta^{\mathrm{c}}|\alpha^{\mathrm{c}} F}{RT}\right) \tag{5}$$

where $k_{\mathrm{s,e,0}}$ is the intrinsic reaction rate coefficient associated with the nature of the surface reaction involving the reactant species, oxygen, lithium ions and electrons. E_0 is the reaction activation energy, i.e., energy barrier to the surface reaction occurrence in the absence of the cathodic overvoltage, (when $|\eta^{\mathrm{c}}| = 0.0$ V), and α^{c} is the charge transfer coefficient across the cathode–electrolyte interface and has a value of 1.0 if it is assumed that 2 electron transfer step is the rate-determining step in the overall intrinsic electrochemical oxygen reduction mechanism. α^{c} is equal to 0.5 for an assumed one electron transfer rate-determining step.

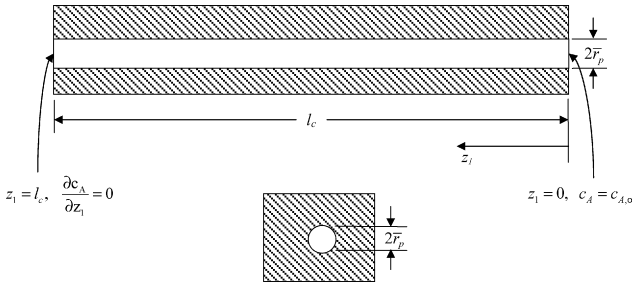

Fig. 2. Schematic of an individual pore in the cathode reaction layer.

It is here assumed that there are n_{p} open-ended pores, each of mean pore radius, $\bar{r}_{\mathrm{p}}$, corresponding to a unit geometric area perpendicular to the z_1 coordinate (see Fig. 2). The initial pore volume in the cathode reaction layer just before the start of the oxygen reduction process per unit geometric area perpendicular to the z_1 coordinate is given by

$$(\pi\bar{r}_{\mathrm{p,0}}^2 \tau l_{\mathrm{c}}) n_{\mathrm{p}} = l_{\mathrm{c}}\varepsilon_0 \tag{6a}$$

The pore volume in the cathode reaction layer during the oxygen reduction process is given by

$$(\pi\bar{r}_{\mathrm{p}}^2 \tau l_{\mathrm{c}}) n_{\mathrm{p}} = l_{\mathrm{c}}\varepsilon \tag{6b}$$

Division of Eq. (6b) by Eq. (6a) leads to

$$\varepsilon = \varepsilon_0\left(\frac{\bar{r}_{\mathrm{p}}}{\bar{r}_{\mathrm{p,0}}}\right)^2 \tag{7}$$

where ε_0 and $\bar{r}_{\mathrm{p,0}}$ are the cathode void fraction and mean pore radius, respectively, just before the start of the oxygen reduction process, and, ε and $\bar{r}_{\mathrm{p}}$ are the cathode void fraction and mean pore radius, respectively, at any time during the oxygen reduction process. It is assumed that the oxygen mass diffusivity in the liquid phase electrolyte and the pore tortuosity are constant. The following dimensionless quantities are now defined as:

$$r = \frac{\bar{r}_{\mathrm{p}}}{\bar{r}_{\mathrm{p,0}}} \tag{8a}$$

$$c_{\mathrm{A,d}} = \frac{c_{\mathrm{A}}}{c_{\mathrm{A,0}}} \tag{8b}$$

$$\xi = \frac{z_1}{l_{\mathrm{c}}} \tag{8c}$$

where $C_{\mathrm{A,0}}$ is the oxygen molar concentration in the liquid phase electrolyte at the saturation level of dissolved oxygen or at the level of oxygen solubility in the electrolyte in contact with the pure oxygen reactant or air supplied to the cell cathode, l_{c} is the thickness of the porous cathode, and r, $c_{\mathrm{A,d}}$, and ξ are the dimensionless pore radius, oxygen concentration, and distance along the z_1 coordinate increasing towards the protective anode, respectively. Substituting for R_{A} and ε from Eqs. (4) and (7),

respectively, into Eq. (3), and expressing $\bar{r}_p$, c_A, and z_1 in terms of the dimensionless quantities, the following continuity equation for oxygen in the dimensionless form is obtained

$$\frac{\partial(r^2 c_{A,d})}{\partial t'} = \frac{\partial}{\partial \xi}\left(r^2 \frac{\partial c_{A,d}}{\partial \xi}\right) - \beta(r c_{A,d}) \tag{9}$$

where

$$t' = \frac{t D_A}{\tau l_c^2} \tag{9a}$$

and

$$\beta = \frac{2 k_s \tau l_c^2}{D_A \bar{r}_{p,0}} \tag{9b}$$

The rate of decrease of pore volume per unit total porous cathode volume due to the formation of solid $Li_2O_{2(s)}$ via the overall reaction, $2Li^+ + 2e^- + O_2 \rightleftharpoons Li_2O_{2(s)}$, is given by

$$\frac{\partial \varepsilon}{\partial t} = -R_A \frac{M_{Li_2O_2}}{\rho_{Li_2O_{2(s)}}} \tag{10}$$

Substitution for R_A and ε from Eqs. (4) and (7), respectively, into Eq. (10), and further simplification leads to

$$\frac{\partial \bar{r}_p}{\partial t} = -\frac{k_s c_A M_{Li_2O_2}}{\rho_{Li_2O_{2(s)}}} \tag{11}$$

Expressing $\bar{r}_p$ and t in the dimensionless form, Eq. (11) becomes

$$\frac{\partial r}{\partial t'} = -\gamma c_{A,d} \tag{12}$$

where

$$\gamma = \frac{(k_s c_{A,0} M_{Li_2O_2}/\rho_{Li_2O_{2(s)}})}{(D_A \bar{r}_{p,0}/\tau l_c^2)} \tag{12a}$$

To solve the coupled differential equations given by Eqs. (9) and (12) for $c_{A,d}$ and r analytically or numerically, the following conditions in the dimensional form are used.

- Initial conditions, $t \le 0$; $0 \le z_1 \le l_c$:

$$\bar{r}_p = \bar{r}_{p,0} \tag{13a}$$

$$c_A = c_A^0 \tag{13b}$$

- Boundary conditions, $t > 0$:

$$z_1 = 0, \qquad c_A = c_{A,0} \tag{14a}$$

$$z_1 = l_c, \qquad \frac{\partial c_A}{\partial z_1} = 0 \tag{14b}$$

The above conditions are turned into the dimensionless form using the quantities given in Eqs. (8a)–(8c).

- Initial conditions, $t' \le 0$; $0 \le \xi \le 1$:

$$r = \frac{\bar{r}_p}{\bar{r}_{p,0}} = 1 \tag{15a}$$

$$c_{A,d} = \frac{c_A^0}{c_{A,0}} \tag{15b}$$

- Boundary conditions, $t' > 0$:
  - at $\xi = 0$

$$c_{A,d} = \frac{c_A}{c_{A,0}} = 1 \tag{16a}$$

  - at $\xi = 1$

$$\frac{\partial c_{A,d}}{\partial \xi} = 0 \tag{16b}$$

Oxygen molar flux into the electrolyte at any time during the cell discharge period, per unit geometric area perpendicular to z_1, is given by

$$\dot{N}_{O_2}|_{z_1=0} = \frac{D_A \varepsilon}{\tau}\left(-\frac{\partial c_A}{\partial z_1}\right)\bigg|_{z_1=0} \tag{17a}$$

On substitution for ε from Eq. (7) into Eq. (17a) and the use of dimensionless quantities, one obtains

$$\dot{N}_{O_2}|_{\xi=0} = \left(\frac{\varepsilon_0 D_A c_{A,0}}{\tau l_c}\right)\left[r^2\left(-\frac{\partial c_{A,d}}{\partial \xi}\right)\right]\bigg|_{\xi=0} \tag{17b}$$

The current generation rate per unit geometric area perpendicular to z_1 in a differential thickness of dz_1, via the occurrence of the electrochemical reaction: $2Li^+ + 2e^- + O_2 \rightleftharpoons Li_2O_{2(s)}$, is given by

$$di_{geom} = 2F R_A \, dz_1 \tag{18}$$

Using the expression for R_A in Eq. (4)

$$di_{geom} = \frac{4F k_s \varepsilon c_A}{\bar{r}_p} \, dz_1 \tag{18a}$$

Substituting for $(\varepsilon/\bar{r}_p)$ from Eq. (7) into Eq. (18a) and using the dimensionless quantities given in Eqs. (8a)–(8c), one obtains

$$di_{geom} = 4F(k_s c_{A,0})\left(\frac{\varepsilon_0 l_c}{\bar{r}_{p,0}}\right) r c_{A,d} \, d\xi \tag{19}$$

Total geometric current density, corresponding to the oxygen reduction reaction occurring in the cathode reaction layer is then given by

$$i_{geom} = \int_0^{i_{geom}} di_{geom} = \left[4F(k_s c_{A,0})\left(\frac{\varepsilon_0 l_c}{\bar{r}_{p,0}}\right)\right]\int_{\xi=0}^{\xi=1} (r c_{A,d}) \, d\xi \tag{20}$$

It should be noted that Eq. (20) gives oxygen reduction geometric current density at any time during the cell discharge. At the end of each time interval, the numerical solution of Eqs. (9) and (12) would provide data on the dimensionless oxygen concentration, $c_{A,d}$, and the dimensionless average pore radius, r, as a function of the dimensionless distance, ξ. Using this data in Eq. (20), one can carry out the integration of Eq. (20) either numerically or graphically to determine the average geometric current density at the end of each time interval. If i_{geom} is to be kept at a constant

Table 2
Parameter values used in simulation

Parameter	Value(s)
l_c	0.001, 0.010, and 0.070 cm
$c_{A,0}$	6.44692E−07 g mol cm^{-3} at 0.2 atm O_2, 1.934076E−06 g mol cm^{-3} at 0.6 atm O_2, 3.22346E−06 g mol cm^{-3} at 1 atm O_2 (all for 1 M $LiPF_6$ in PC/DME)
ε_0	0.73 [4]
D_A	7.00E−6 cm^2 s^{-1} [5]
$\bar{r}_{p,\circ}$	2.00E−7 cm (estimate)
$MW_{Li_2O_2}$	45.8768 g (g mol)$^{-1}$
$\rho_{Li_2O_2}$	2.3 g cm^{-3} [7]
τ	1.17 (calculated from $\tau = \varepsilon_\circ^{-0.5}$)
i_{geom}	5, 1, 0.5, 0.1, 0.05 mA cm^{-2}
T	298.15 K
α	0.0722 [5] for 1 M $LiPF_6$ in PC/DME
α^c	1

level with respect to time, Eq. (20) suggests that the product $\left[k_s \int_0^1 (rc_{A,d})\,d\xi\right]$ must be kept constant. Because $\int_{\xi=0}^{\xi=1} (rc_{A,d})\,d\xi$ is likely to decrease with time; therefore, k_s must be increased to a level so that $\left[k_s \int_0^1 (rc_{A,d})\,d\xi\right]$ = constant with respect to time. From Eq. (20), in conjunction with Eq. (5), i_{geom} is expressed as

$$i_{geom} = \left(4F\frac{\varepsilon_0 l_c}{\bar{r}_{p,0}} c_{A,0}\right)\left(k_{s,e}\exp\left(\frac{|\eta^c|\,\alpha^c F}{RT}\right)\right) \times \int_{\xi=0}^{\xi=1} (rc_{A,d})\,d\xi \quad (21a)$$

The geometric current density at a time, $t = t_1$ or $t' = t_1'$, is given by

$$i_{geom,t_1} = \left(\frac{4F\varepsilon_0 l_c c_{A,0}}{\bar{r}_{p,0}}\right)\left(k_{s,e}\exp\left(\frac{|\eta^c|_{t_1}\alpha^c F}{RT}\right)\right) \times \left[\int_{\xi=0}^{\xi=1} (rc_{A,d})\,d\xi\right]_{t_1} \quad (21b)$$

Division of Eq. (21a) by (21b) leads to

$$\frac{i_{geom}}{i_{geom,t_1}} = \exp\left[(|\eta^c| - |\eta^c|_{t_1})\frac{\alpha^c F}{RT}\right]\left[\frac{\int_0^1 (rc_{A,d})\,d\xi}{\left\{\int_0^1 (rc_{A,d})\,d\xi\right\}_{t_1}}\right] \quad (22)$$

In order that the geometric current density can be kept constant with respect to time, i.e., $(i_{geom}/i_{geom,t_1}) = 1$, it requires that

$$\exp\left[-\frac{(|\eta^c| - |\eta^c|_{t_1})\alpha^c F}{RT}\right] = \frac{\int_0^1 (rc_{A,d})\,d\xi}{\left\{\int_0^1 (rc_{A,d})\,d\xi\right\}_{t_1}} \quad (23)$$

Eq. (23) suggests that if the average geometric current density at any time, t, is to be equal to that at a time, $t = t_1$, where the oxygen reduction overvoltage is $|\eta^c|_{t_1}$; the overvoltage $|\eta^c|$ must be adjusted and equal to that given by Eq. (23). Because the numerator of the right-hand side of Eq. (23) will decrease as the cell discharge time increases; therefore, the cathodic reaction overvoltage, $|\eta^c|$, should increase with time to maintain the geometric current density at a desired constant level.

3. Results and discussion

Under numerically constant geometric current density and oxygen solubility in the organic electrolyte solution, Eqs. (9) and (10) were solved numerically using an explicit finite difference technique. The relationship in Eq. (23) was used to keep i_{geom} constant by arbitrarily setting $|\eta^c|_{t_1} = 0$ and for the initial conditions used knowing that the integral on the bottom of the right-hand side of Eq. (23) is equal to 1.0. Table 2 lists the parameters used in the simulation.

Fig. 3 shows the dimensionless pore radius as a function of percent of total pore length and dimensionless time for a geometric current density of 0.5 mA cm^{-2}, a cathode thickness of 0.070 cm and an oxygen partial pressure of 1.0 atm. The highest dimensionless time represents the total discharge time for the cell. The simulated discharge would end when the relationship provided by Eq. (23) "blew-up", that is, there was not enough dissolved oxygen to sustain the needed current. Fig. 4 has the same parameters as Fig. 3 except the geometric current density is 0.10 mA cm^{-2}. Note that at the lower current density, as shown by Fig. 4 in comparison to Fig. 3, a higher utilization of the electrode is realized as shown by the lower steepness

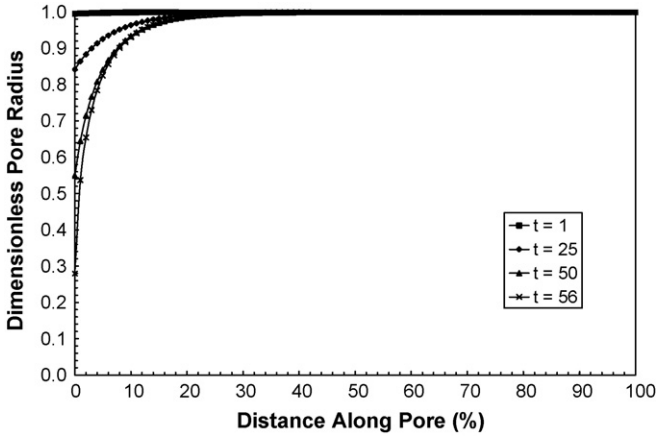

Fig. 3. Dimensionless pore radius versus pore distance for $i_{geom} = 0.5$ mA cm^{-2}, $l_c = 0.07$ cm and O_2 partial pressure = 1.0 atm.

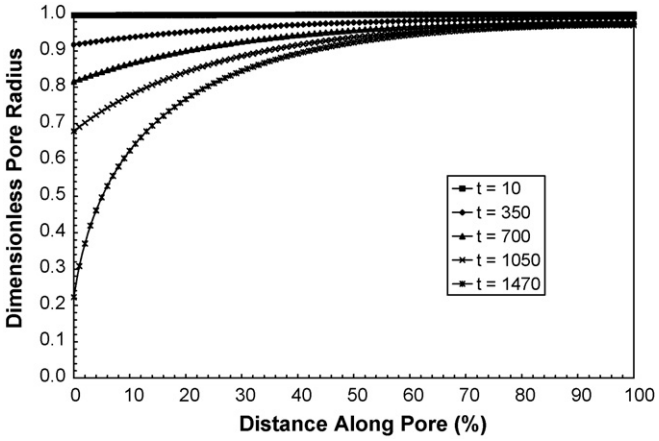

Fig. 4. Dimensionless pore radius vs. pore distance for $i_{geom} = 0.1\ mA\ cm^{-2}$, $l_c = 0.07$ cm and O_2 partial pressure = 1.0 atm.

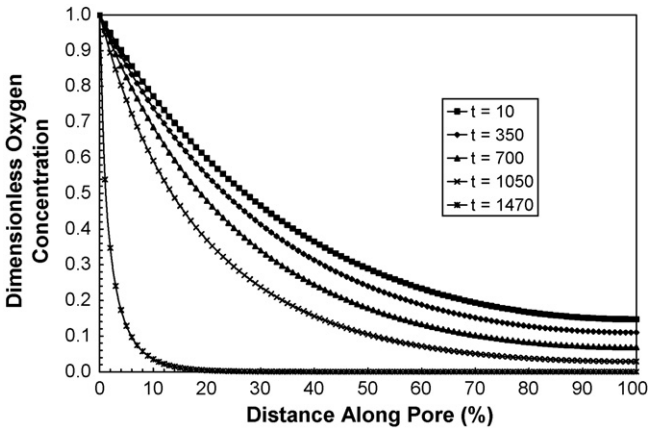

Fig. 6. Dimensionless oxygen concentration vs. pore distance for $i_{geom} = 0.1\ mA\ cm^{-2}$, $l_c = 0.07$ cm and O_2 partial pressure = 1.0 atm.

of the dimensionless pore radius versus the dimensionless pore axial distance profile. Also note that the pore radius gradient in Fig. 4 is less than that for Fig. 3 due to the lower current density.

With respect to Figs. 3 and 4, Figs. 5 and 6 show the corresponding dimensionless oxygen concentration profiles in the pores. Note that the concentration gradient in Fig. 5 is higher than Fig. 6 due to the higher current density. Also, the oxygen concentration limiting the discharge time is clearly evident in Figs. 5 and 6.

To determine the specific capacities ($mAh\ g^{-1}$ of carbon) of the modeled cell, as a first approximation it was assumed that the solid volume fraction of the cathode, 0.27, was initially composed of only the carbon material with its density in the cathode being $2.2\ g\ cm^{-3}$. Fig. 7 shows the cell specific capacity as a function of oxygen partial pressure and geometric current densities. This curve is very similar to measured experimental values (see Fig. 3 in [5]).

Fig. 8 shows the specific capacity as a function of geometric current density and cathode thickness for this pore flooded-electrolyte design. Clearly, as the cathode thickness is reduced,

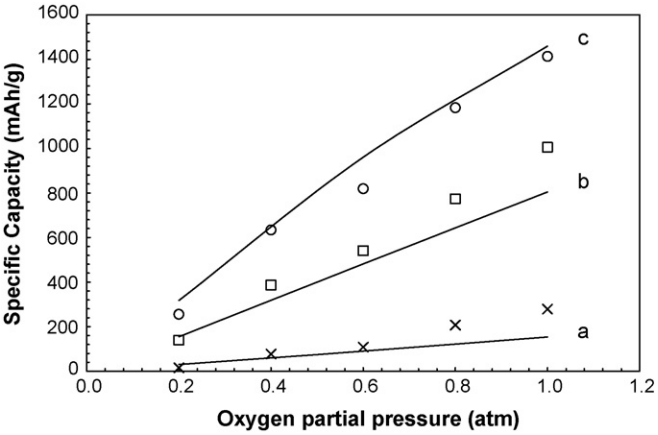

Fig. 7. Lines are the calculated specific capacities ($mAh\ g^{-1}$ of carbon) for $l_c = 0.07$ cm as a function of oxygen partial pressure and current densities of (a) 0.5, (b) 0.1, and (c) $0.05\ mA\ cm^{-2}$. Symbols are the experimental values from Fig. 3 in [5].

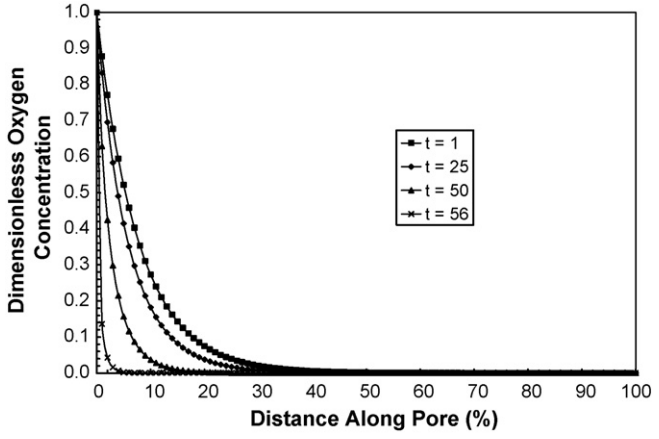

Fig. 5. Dimensionless oxygen concentration vs. pore distance for $i_{geom} = 0.5\ mA\ cm^{-2}$, $l_c = 0.07$ cm and O_2 partial pressure = 1.0 atm.

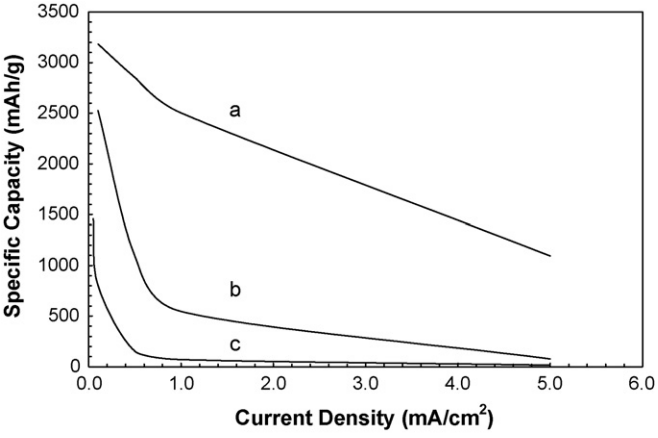

Fig. 8. Specific capacity ($mAh\ g^{-1}$ of carbon) as a function of current density for an oxygen partial pressure of 1.0 atm and l_c's of (a) 0.001, (b) 0.01, and (c) 0.07 cm.

the cell performance as measured in terms of specific capacity for a given current density is greatly enhanced.

It has clearly been shown above by simulation that Read's [4,5] lithium/oxygen cells were flooded with electrolyte. The simulations represented by Fig. 7 are closely correlated with experimental results under the same conditions. Fig. 8 shows that thick cathode cell designs are not optimal and that a trade-off between starved and flooded electrolyte cell designs also needs to be performed.

4. Conclusions

A diffusion-limited model for lithium/air battery with an organic electrolyte was developed and the results from the model compare favorably with experimental results. The model shows, for a given cathode pore radius, the effect of oxygen partial pressure, current density, and cathode thickness on the specific capacity of the battery.

References

[1] K.M. Abraham, Z. Jiang, A polymer electrolyte-based rechargeable lithium/oxygen battery, J. Electrochem. Soc. 143 (1996) 1–5.
[2] DOE, Properties of Fuels, http://www.eere.energy.gov/afdc/pdfs/fueltable.pdf, 2006.
[3] A. Dobley, R. Rodriguez, K.M. Abraham, Abstract No. 496, High Capacity Cathodes for Lithium–Air Batteries, Electrochem Society Joint International Meeting, Electrochem. Soc., 2004.
[4] J. Read, Characterization of the lithium/oxygen organic electrolyte battery, J. Electrochem. Soc. 149 (2002) A1190–A1195.
[5] J. Read, K. Mutolo, M. Ervin, W. Behl, J. Wolfenstine, A. Driedger, D. Foster, Oxygen transport properties of organic electrolytes and performance of lithium/oxygen battery, J. Electrochem. Soc. 150 (2003).
[6] T. Ogasawara, A. Debart, M. Holzapfel, P. Novak, P.G. Bruce, Rechargeable Li_2O_2 electrode for lithium batteries, J. Am. Chem. Soc. 128 (2006) 1390–1393.
[7] S.S. Sandhu, G.W. Brutchen, J.P. Fellner, Lithium–air battery system: preliminary analysis, in: Proceedings of the 13th International Conference on Electrical and Electronic Products, Product Safety Corporation, Sissonville, West Virginia, 2006.